Radiomic model of contrast-enhanced computed tomographyfor predicting liver injury in acute pancreatitis patients

Lu Liu
Affiliated Hospital of North Sichuan Medical College
Ningjun Yu
Affiliated Hospital of North Sichuan Medical College
Tingting Liu
Affiliated Hospital of North Sichuan Medical College
Shujun Chen
Affiliated Hospital of North Sichuan Medical College
Yu Pu
Affiliated Hospital of North Sichuan Medical College
Wei Tang
Affiliated Hospital of North Sichuan Medical College
Yong Li
Affiliated Hospital of North Sichuan Medical College
Xiaoming Zhang (zhangxm@nsmc.edu.cn)
Affiliated Hospital of North Sichuan Medical College
Xinghui Li
Affiliated Hospital of North Sichuan Medical College

Research Article

Keywords: Radiomics, acute pancreatitis (AP), liver injury, contrast-enhanced computed tomography (CECT)

Posted Date: January 22nd, 2024

DOI: https://doi.org/10.21203/rs.3.rs-3844424/v1

Additional Declarations: No competing interests reported.

Abstract

Objectives

To predict liver injury in acute pancreatitis (AP) patients by establishing a radiomics model based on contrast-enhanced computed tomography (CECT).

Methods

A total of 1223 radiomic features were extracted from late arterial-phase pancreatic CECT images of 209 AP patients (146 in the training cohort and 63 in the test cohort), and the optimal radiomic features retained after dimensionality reduction by least absolute shrinkage and selection operator (LASSO) were used to construct a radiomic model through logistic regression analysis. In addition, clinical features were collected to develop a clinical model, and a joint model was established by combining the best radiomic features and clinical features to evaluate the practicality and application value of the radiomic models, clinical model and combined model.

Results

Four potential features were selected from the pancreatic parenchyma to construct the radiomic model, and the area under the receiver operating characteristic curve (AUC) of the radiomic model was significantly greater than that of the clinical model for both the training cohort (0.993 vs. 0.653, p = 0.000) and test cohort (0.910 vs. 0.574, p = 0.000). The joint model had a greater AUC than the radiomics model for both the training cohort (0.997 vs. 0.993, p = 0.357) and test cohort (0.925 vs. 0.910, p = 0.302).

Conclusions

The radiomic model based on CECT has good performance in predicting liver injury in AP patients and can guide clinical decision-making and improve the prognosis of patients with AP.

1. Introduction

Acute pancreatitis (AP) is a potentially fatal inflammatory disease of the digestive system characterized by the activation of pancreatic enzymes with varying degrees of edema, hemorrhage, and necrosis(1, 2). Its course is rapidly progressive, and patients are prone to develop moderate AP or severe AP, leading to pancreatic necrosis, systemic inflammatory response syndrome, and multiple-organ dysfunction syndrome, all of which are associated with a high mortality rate(3, 4). Acute liver injury (ALI) is the most common complication of AP and is associated with liver function impairment, the probability of which can reach 60% due to a systemic inflammatory response, a decrease in the circulating blood volume, or the special anatomical structure of the liver and pancreas(5–7). Severe progression to hepatic failure

occurs with a 5% incidence, leading to death(8). In addition, AP complicated with liver injury can not only accelerate the progression of the disease but also play a bridging role in the process of multiple-organ injury secondary to AP(9). Therefore, early diagnosis and treatment of liver injury can effectively improve the prognosis and survival rate of AP patients.

Currently, the commonly used method for the clinical diagnosis of AP complicated with liver injury is laboratory examination, but laboratory examination cannot accurately and intuitively evaluate the severity of AP (such as necrosis and effusion) or guide clinicians to treat patients individually. Contrast-enhanced computed tomography (CECT) is the recommended imaging method for the diagnosis of pancreatic and hepatic diseases, but early liver injury only shows transient hepatic attenuation differences on CECT images(10), which lacks specificity and makes an accurate diagnosis difficult with the naked eye.

As an emerging technology, radiomics is a noninvasive method for extracting quantitative features in a high-throughput manner, discovering information about the heterogeneity of lesions that cannot be observed by the naked eye, improving the diagnostic rate of diseases, and providing support for clinical decision-making(11, 12).Radiomics has important applications in predicting the severity of AP, the recurrence of AP, the incidence of early extrapancreatic necrosis in AP patients and post-AP diabetes mellitus and has achieved good results(13–15). However, there are no radiomic reports on AP complicated with liver injury. Therefore, the aim of this paper was to develop a predictive model based on CECT for diagnosing ALI in AP patients.

2. Materials and methods

2.1 Patients

This retrospective study was approved by the Medical Ethics Committee of the Affiliated Hospital of North Sichuan Medical College. The ethics committee's approval number for this experiment was [2021] 08, and the study was exempted from informed consent requirements. In this study, the medical records of 658 AP patients admitted to the Affiliated Hospital of North Sichuan Medical College from January 2019 to December 2022 were collected.

2.2 Inclusion and exclusion criteria

The inclusion criteria for patients were as follows: (I) had AP according to the Atlanta classification revised in 2012(16); (II) had serum liver function indices, including alanine aminotransferase (ALT), aspartate aminotransferase (AST), total bilirubin (TBIL) and direct bilirubin (DBIL), within 48 h after the onset of the disease in AP patients; and (III) had abdominal CT enhancement scans performed within 2 days after onset.

The exclusion criteria were as follows: (I) incomplete medical history; (II) poor-quality CECT images; (III) acute exacerbation of chronic pancreatitis; (IV) previous history of liver injury; (V) recent administration of

liver damaging medications; and (VI) comorbid infectious diseases and pancreatic tumors.

A total of 209 AP patients were ultimately included in the study. According to the indices of laboratory liver function, the patients were divided into a liver injury group (n = 94) and a nonliver injury group (n = 115). The training cohort (n = 146, 76 in the nonliver injury group and 70 in the liver injury group) and the test cohort (n = 63, 36 in the nonliver injury group and 27 in the liver injury group) were randomly generated by R software according to a ratio of 7:3. In addition, information such as sex, age, etiology, complications, hospital stay, hydroperitoneum, fatty liver disease status, modified computed tomography severity index (MCTSI) score (Table 1), bedside index for severity in AP (BISAP) score(17), Acute Physiology and Chronic Health Evaluation (APACHE) II score(18), AP severity based on the Atlanta Classification Criteria(16), biochemical indices of pancreatitis (serum amylase, serum pancreatic amylase and lipase) and serum liver function indices (ALT, AST, TBIL, DBIL) was collected. The flowchart of the recruitment of patients is shown in Fig. 1.

Table 1
Composition of the severity scores on the MCTSI.

Characteristics	Score
Pancreatic inflammation	
Normal	0
Focal or diffuse enlargement	2
Intrinsic pancreatic abnormalities with inflammatory changes in pancreatic fat	2
Single, poorly defined fluid collection or phlegmon	4
2 or more poorly defined collection or presence of gas in or adjacent to pancreas	4
pancreatic necrosis	
None	0
<30%	2
30%-50%	4
>30%	4
Extrapancreatic complications	2
Ascites, pleural effusion, gastrointestinal tract involvement, vascular complications, parenchymal complications	

2.3 Image acquisition

All AP patients were scanned by a Somatom Definition AS + 128 (Siemens Healthineers). The scanning parameters were as follows: 120 kV tube voltage, 200 mA tube current, 512 × 512 matrix, 35 cm × 35 cm

field of view, 128 × 0.6 mm detector collimation, 5 mm section thickness, and 5 mm section interval. Using a high-pressure syringe, 1.5 mL/kg of nonionic contrast agent was injected intravenously in an elbow vein at a rate of 3.5-4 mL/s and then flushed with 10 mL of saline solution. Images of the arterial and portal venous phases were acquired 28 and 60 seconds after injection, respectively. Arterial phase CT images were anonymously retrieved from a picture archiving and communication system (PACS) (Carestream) for feature extraction.

2.4 Region of interest (ROI) delineation, image segmentation, and feature extraction

Two experienced abdominal radiologists manually delineated the ROI of the pancreatic parenchyma in the arterial phase with the three-dimensional (3D) Slicer (https://www.slicer.org/) platform layer by layer, including the pancreatic necrosis area, vessels and biliary ducts were avoided as much as possible. The original image was resampled and filtered by Laplace-Gaussian filtering and wavelet transform filtering based on the 3D slicer platform, and the radiomics features were extracted to obtain 1223 features, including seven groups of features, including the first-order features, shape features, gray level size zone matrix (GLSZM), neighboring gray-tone difference matrix (NGTDM), gray level dependence matrix (GLDM), gray level co-occurrence matrix (GLCM), and gray level run-length matrix (GLRLM).

2.5 Intraobserver and interobserver agreement

To assess intraobserver reliability and interobserver agreement, two abdominal radiologists randomly selected arterial-phase images from 50 patients to delineate ROIs and extract features. For intraobserver reliability, observer 1 delineated the ROI twice in one week, and the radiomic features were extracted twice. To assess interobserver agreement, observer 2 delineated the ROI and extracted features for comparison with the extracted features of observer 1. Agreement between the intra- and interobserver distributions was assessed using the intragroup correlation coefficient (ICC), and features with an ICC greater than 0.75 were considered to indicate good agreement(19).

2.6 Dimensionality reduction and radiomic feature selection

Features with an ICC greater than 0.75 were normalized by the Z score to eliminate the dimensional effects associated with different features. The features of the training cohort were subsequently tested by the independent samples t test or the Mann—Whitney U test to avoid dimension bias. Finally, variable selection and regularization were performed by least absolute shrinkage and selection operator (LASSO) to obtain the best radiomic features associated with liver injury. In this study, the regularization parameter (λ) was adjusted, and tenfold cross-validation was used to select features and determine the corresponding coefficient values to weigh these features. The workflow of the radiological analysis is shown below: Fig. 2.

2.7 Establishment of the clinical model and radiomic model

The clinical features of the liver injury group and the nonliver injury group were analyzed by univariate analyses, and a clinical model was constructed based on the clinical features that differed between the two groups. A radiomic model was created from the best radiomic features screened after dimensionality reduction, and the model was evaluated based on specificity, sensitivity, precision, accuracy, recall, F1 score, and the area under the receiver operating characteristic curve (AUC). In addition, the difference in AUC values between the two models was also calculated to determine the best model for predicting liver injury in AP patients.

2.8 Statistical analysis

All the data were analyzed with SPSS 27.0 (IBM). The normality of the distribution of continuous variables was assessed using the Shapiro–Wilk test, and the Levene test was used to test for homogeneity of variance. Independent t tests were used for continuous variables that conformed to a normal distribution, and Mann–Whitney U tests were used for continuous variables that did not conform to a normal distribution. The chi-square test or Fisher's exact test was used to test categorical variables. The difference in AUC values between the two models was compared by the Delong test, and $p < 0.05$ was considered to indicate a significant difference.

3. Results

3.1 Clinical characteristics

A total of 209 patients with AP were included in this study. According to the Atlanta Classification criteria, 86 patients had mild AP, 101 had moderate AP, and 22 had severe AP; 94 patients were included in the liver injury group, and 115 patients were included in the non-liver injury group (Fig. 3). The clinical characteristics of the two groups are summarized in Table 1. The results revealed significant differences in age; APACHE II score; lipase level; serum amylase level; and serum pancreatic amylase level between the two groups.

Table 2
Clinical characteristics of the liver injury group and nonliver injury group

Clinical characteristics	Liver injury group (n = 94)	Nonliver injury group (n = 115)	P value
Gender			0.863
Male	64	77	
Female	30	38	
Age (years)	50.97 ± 15.27	46.95 ± 14.84	0.043
Etiology			0.209
Biliary	38	36	
Alcoholic	6	5	
Hypertriglyceridemia	27	49	
Others	23	25	
Complications			0.555
Yes	48	54	
No	46	61	
MCTSI score	6(2–6)	6(2.5-6)	0.609
BISAP score	1(0–2)	1(0–2)	0.870
APACHE II score	5.5(3–8)	5(2–7)	0.021
Fatty liver disease			0.602
Yes	44	57	
No	50	58	
Hydroperitoneum			0.114
Yes	73	78	
No	21	37	
Hospital stay (days)	10(6–14)	12(8–16)	0.06
Lipase	356(121–841)	482(189-1461.5)	0.018
Serum amylase	334(121-1382.75)	272(102–566)	
Pancreatic amylase	263(85-1343)	222(81–509)	0.044
AP severity			0.466
Mild	37	49	

Clinical characteristics	Liver injury group (n = 94)	Nonliver injury group (n = 115)	P value
Moderate	45	56	
Severe	12	10	

3.2 Radiomics feature selection

For each patient, 1223 features were extracted, and a total of 805 features with intraobserver and interobserver ICCs > 0.75 were selected (Fig. 4). Independent t tests and Mann–Whitney U tests were used to screen out the features with significant differences, and the four most important features were subsequently selected by LASSO (Fig. 5). The corresponding coefficients for the features are shown in Table 2.

Table 3
The corresponding coefficients for the features identified by LASSO. GLRLM, gray-level run-length matrix; GLDM, gray-level dependence matrix; GLSZM, gray-level size zone matrix.

Category	Feature	Coefficients
GLDM	SmallDependenceHighGrayLevelEmphasis	0.601445
GLRLM	ShortRunHighGrayLevelEmphasis	0.800737
GLSZM	SmallAreaHighGrayLevelEmphasis	-1.021515
GLRLM	RunLengthNonUniformity	0.100813

3.3 Establishment of the clinical model, radiomic model and joint model

A radiomic model was established by logistic regression, a clinical model was built based on five statistically significant clinical features, and a joint model was built based on clinical features and radiomic features. The performance of the clinical model, the radiomic model and the joint model is shown in Table 3. In the training and test cohorts, the areas under the curve (AUCs) of the radiomics model were 0.993 and 0.910, respectively (Fig. 6), which were greater than those of the clinical model (Fig. 7). In addition, the joint model also had a greater AUC than the radiomics model.

Table 4
The performance of the clinical model, radiomic model and joint model in the training and test cohorts. PPV, positive predictive value; NPV, negative predictive value; AUC, area under the receiver operating characteristic curve.

	Accuracy	Sensitivity	Specificity	PPV	NPV	F1	AUC (95% CI)
Training cohort							
Clinical model	0.630	0.500	0.750	0.648	0.620	0.565	0.653(0.564 ~ 0.743)
Radiomics model	0.979	0.986	0.974	0.972	0.987	0.979	0.993 (0.981 ~ 1)
Joint model	0.986	0.986	0.987	0.986	0.987	0.986	0.997 (0.992 ~ 1)
Test cohort							
Clinical model	0.635	0.370	0.833	0.625	0.638	0.465	0.574(0.419 ~ 0.729)
Radiomics model	0.937	0.963	0.917	0.897	0.971	0.929	0.910 (0.818 ~ 1)
Joint model	0.921	0.926	0.917	0.893	0.943	0.909	0.925(0.846 ~ 1)

4. Discussion

Early diagnosis of liver injury caused by AP is important for determining the treatment and prognosis of patients. Several studies have explored different types of liver injury based on radiomics. Fu et al. developed a predictive model based on hepatic enhancement magnetic resonance imaging that incorporated clinical characteristics and radiomic features for predicting chronic drug-induced liver injury(20). The model had high efficacy in the training cohort (AUC = 0.89) and the validation cohort (AUC = 0.88). Guido's group improved the noninvasive diagnosis of chemotherapy-associated liver injury by radiomic analysis of liver parenchyma with high accuracy in diagnosing nonalcoholic steatohepatitis, sinusoidal dilatation, and nodular regenerative hyperplasia(21). Benjamin and his colleagues reported that liver spontaneous attenuation (LSA), which reflects the degree of steatosis on CT, correlates with the clinical severity of AP and that the LSA can serve as an imaging biomarker of AP severity(22). Although there are many studies on liver injury based on radiomics, there is a lack of development and verification of radiomic models for diagnosing AP complicated with liver injury; therefore, we constructed a CT radiomic model based on machine learning. In terms of grouping, we used any ALT, AST, TBIL or DBIL concentration above the normal range to define liver injury. To ensure the accuracy of both the TBIL and DBIL levels, we excluded patients with elevated TBIL and DBIL levels due to biliary obstruction. The results showed that the accuracy of the radiomic model reached 0.979 and 0.937 in the training and test sets, respectively. The four metrics were shown to be highly efficacious in defining liver injury.

In terms of imaging data acquisition, first, CECT is one of the recommended imaging techniques for diagnosing AP and can distinguish local complications(16). In addition, images of the late artery reportedly have the best enhancement effect; therefore, we chose images of the late artery for visualization(23). Second, all AP patients were scanned with the same machine and parameters, ensuring highly reproducible and accurate data. The features were then resampled to 1 × 1 × 1 mm during feature extraction to correct for voxel resolution changes. Finally, after extracting the features, the size effect associated with different features was removed by normalizing the Z score. This series of measures ensures that our data have high conviction.

For feature dimensionality reduction, we used the LASSO algorithm to filter features. Its principle is to reduce the dimensionality of the dataset by selecting the most important features to achieve a higher model accuracy and a faster calculation speed(24). In this study, we optimized the features by adjusting the regularization parameter via the LASSO algorithm and performing 10-fold cross-validation to filter out the four most important features and ensure the stability of the radiomic model. Compared to other studies of liver injury, our model has greater efficacy(20, 21).

This study has several limitations. First, our study was a single-center study with a small sample size. In the future, large-scale multicenter studies can be conducted as much as possible. Second, the reason for the low efficacy of the clinical model may be that the number of patients included was small and unrepresentative, and additional clinical features were not included. Third, only drawing the pancreatic parenchyma may ignore valuable information about the disease. In future research, edema and exudate can be included in the delineation of ROIs to improve diagnostic efficiency.

5. Conclusion

Radiomics has important applications in the study of liver injury in AP patients based on late arterial images from CECT. We developed a powerful radiomic model that can accurately diagnose liver injury in AP patients, providing a new approach for the assessment of liver injury as well as patient prognosis and personalized treatment. Given the noninvasive and efficient nature of radiomics, radiomics can be applied in the future to diagnose multiple complications of AP.

Abbreviations

AP
Acute pancreatitis
CECT
Contrast-enhanced computed tomography
APACHE
Acute Physiology and Chronic Health Evaluation
AUC
Receiver operating characteristic curve

MRSI
MR severity index
ALT
Alanine aminotransferase
AST
Aspartate aminotransferase
TBIL
Total bilirubin
DBIL
Direct bilirubin
ROI
Region of interest
3D
Three-dimensional
ICC
Intragroup correlation coefficient
LASSO
Least absolute shrinkage and selection operator
GLDM
Gray level dependence matrix
NGTDM
Neighboring gray-tone difference matrix
GLSZM
Gray level size zone matrix
GLCM
Gray level co-occurrence matrix
GLRLM
Gray level run-length matrix
LSA
Liver spontaneous attenuation
NPV
Negative predictive value
PPV
Positive predictive value
MCTSI
Modified computed tomography severity index
BISAP
Bedside index for severity in AP

Declarations

Founding

This study was supported by the General Programs of National Natural Science Foundation of China (81871440), the Youth Program of Natural Science Foundation of Sichuan Provincial Department of Science and Technology (2023NSFSC1535), and the Affiliated Hospital of North Sichuan Medical College (2022JB001, BS20211116).

Author information

Lu Liu and Ningjun Yu have contributed equally to this work.

Authors and Affiliations

Medical Imaging Key Laboratory of Sichuan Province, Department of Radiology, Affiliated Hospital of North Sichuan Medical College, 1 South Maoyuan Street, Nanchong 637001, China.

Lu Liu, Ningjun Yu, Tingting Liu, Shujun Chen, Yu Pu, Wei Tang, Yong Li, Xiaoming Zhang*, Xinghui Li*

Corresponding author

Correspondence to Xiaoming Zhang, Xinghui Li.

Conflict of interest

The authors declare that they have no competing interests

Ethical approval

This study was performed in line with the principles of the Declaration of Helsinki and approved by the Medical Ethics Committee of the Affiliated Hospital of North Sichuan Medical College (Approval Number [2021] 08).

Author Contribution

Manuscript writing/editing: L.L., X.L., X.Z. Data collection and management: N.Y., L.L. Protocol/project development: X.L., L.L., W.T., Y.P., Y.L. Data analysis: L.L., N.Y., T.L., S.J. All authors read and approved the final manuscript.

References

1. Lankisch PG, Apte M, Banks PA. Acute pancreatitis. Lancet. 2015;386(9988):85–96.
2. Saluja A, Dudeja V, Dawra R, Sah RP. Early Intra-Acinar Events in Pathogenesis of Pancreatitis. Gastroenterology. 2019;156(7):1979–93.

3. Schepers NJ, Bakker OJ, Besselink MG, Ahmed Ali U, Bollen TL, Gooszen HG, et al. Impact of characteristics of organ failure and infected necrosis on mortality in necrotising pancreatitis. Gut. 2019;68(6):1044–51.
4. van Dijk SM, Hallensleben NDL, van Santvoort HC, Fockens P, van Goor H, Bruno MJ, et al. Acute pancreatitis: recent advances through randomised trials. Gut. 2017;66(11):2024–32.
5. Wang X, Zhao X, Shi C, Börjesson A, Chen Z, Axelsson J, et al. Potential mechanisms and significance of acute pancreatitis-associated liver injury. Scandinavian Journal of Gastroenterology. 2009;41(5):604–13.
6. Manrai M, Kochhar R, Gupta V, Yadav TD, Dhaka N, Kalra N, et al. Outcome of Acute Pancreatic and Peripancreatic Collections Occurring in Patients With Acute Pancreatitis. Annals of Surgery. 2018;267(2):357–63.
7. Folch-Puy E. Importance of the liver in systemic complications associated with acute pancreatitis: the role of Kupffer cells. The Journal of Pathology. 2007;211(4):383–8.
8. Kyösola K, Fock G. Complications in acute pancreatitis. Ann Chir Gynaecol. 1976;65(1):7–12.
9. Wang Y, Liu W, Liu X, Sheng M, Pei Y, Lei R, et al. Role of Liver in Modulating the Release of Inflammatory Cytokines Involved in Lung and Multiple Organ Dysfunction in Severe Acute Pancreatitis. Cell Biochemistry and Biophysics. 2014;71(2):765–76.
10. Arita T MN, Takano K, Hara A, Fujita T, Honjo K. Hepatic perfusion abnormalities in acute pancreatitis: CT appearance and clinical importance. Abdom Imaging. 1999;24(2):157–62.
11. Lambin P, Rios-Velazquez E, Leijenaar R, Carvalho S, van Stiphout RGPM, Granton P, et al. Radiomics: Extracting more information from medical images using advanced feature analysis. European Journal of Cancer. 2012;48(4):441–6.
12. Mayerhoefer ME, Materka A, Langs G, Häggström I, Szczypiński P, Gibbs P, et al. Introduction to Radiomics. Journal of Nuclear Medicine. 2020;61(4):488–95.
13. Zhou T, Xie C-l, Chen Y, Deng Y, Wu J-l, Liang R, et al. Magnetic Resonance Imaging–Based Radiomics Models to Predict Early Extrapancreatic Necrosis in Acute Pancreatitis. Pancreas. 2021;50(10):1368–75.
14. Zhao Y, Wei J, Xiao B, Wang L, Jiang X, Zhu Y, et al. Early prediction of acute pancreatitis severity based on changes in pancreatic and peripancreatic computed tomography radiomics nomogram. Quantitative Imaging in Medicine and Surgery. 2023;13(3):1927–36.
15. Chen Y, Chen T-w, Wu C-q, Lin Q, Hu R, Xie C-l, et al. Radiomics model of contrast-enhanced computed tomography for predicting the recurrence of acute pancreatitis. European Radiology. 2018;29(8):4408–17.
16. Banks PA, Bollen TL, Dervenis C, Gooszen HG, Johnson CD, Sarr MG, et al. Classification of acute pancreatitis–2012: revision of the Atlanta classification and definitions by international consensus. Gut. 2013;62(1):102–11.
17. Sastre J, Gao W, Yang H-X, Ma C-E. The Value of BISAP Score for Predicting Mortality and Severity in Acute Pancreatitis: A Systematic Review and Meta-Analysis. Plos One. 2015;10(6).

18. Simoes. Predicting Acute Pancreatitis Severity: Comparison of Prognostic Scores. Gastroenterology Research. 2011.
19. Shafiq-ul-Hassan M, Zhang GG, Latifi K, Ullah G, Hunt DC, Balagurunathan Y, et al. Intrinsic dependencies of CT radiomic features on voxel size and number of gray levels. Medical Physics. 2017;44(3):1050–62.
20. Fu H, Shen Z, Lai R, Zhou T, Huang Y, Zhao S, et al. Clinic-radiomics model using liver magnetic resonance imaging helps predict chronicity of drug-induced liver injury. Hepatology International. 2023;17(6):1626–36.
21. Costa G, Cavinato L, Masci C, Fiz F, Sollini M, Politi LS, et al. Virtual Biopsy for Diagnosis of Chemotherapy-Associated Liver Injuries and Steatohepatitis: A Combined Radiomic and Clinical Model in Patients with Colorectal Liver Metastases. Cancers. 2021;13(12).
22. Roussey B, Calame P, Revel L, Zver T, Konan A, Piton G, et al. Liver spontaneous hypoattenuation on CT is an imaging biomarker of the severity of acute pancreatitis. Diagnostic and Interventional Imaging. 2022;103(9):401–7.
23. Kanematsu M SY, Hoshi H, Kondo H, Matsuo M, Moriwaki H. Pancreas and peripancreatic vessels: effect of imaging delay on gadolinium enhancement at dynamic gradient-recalled-echo MR imaging. Radiology. 2000;215(1).
24. Tibshirani R. Regression shrinkage and selection via the lasso. Journal of the Royal Statistical Society Series B (Methodological). 2018;58:267–88.

Figures

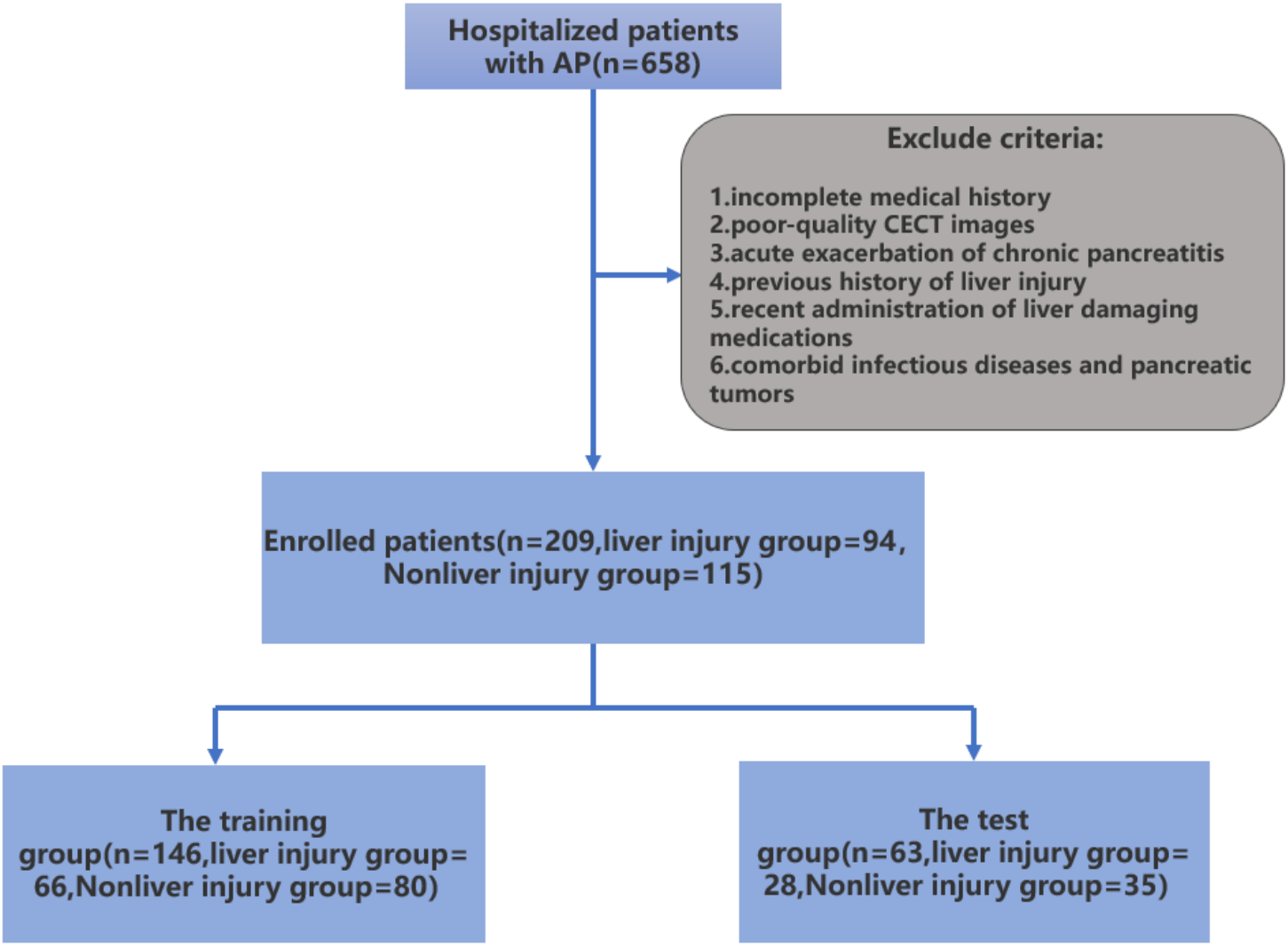

Figure 1

Flow chart of patient recruitment in this study. AP, acute pancreatitis.

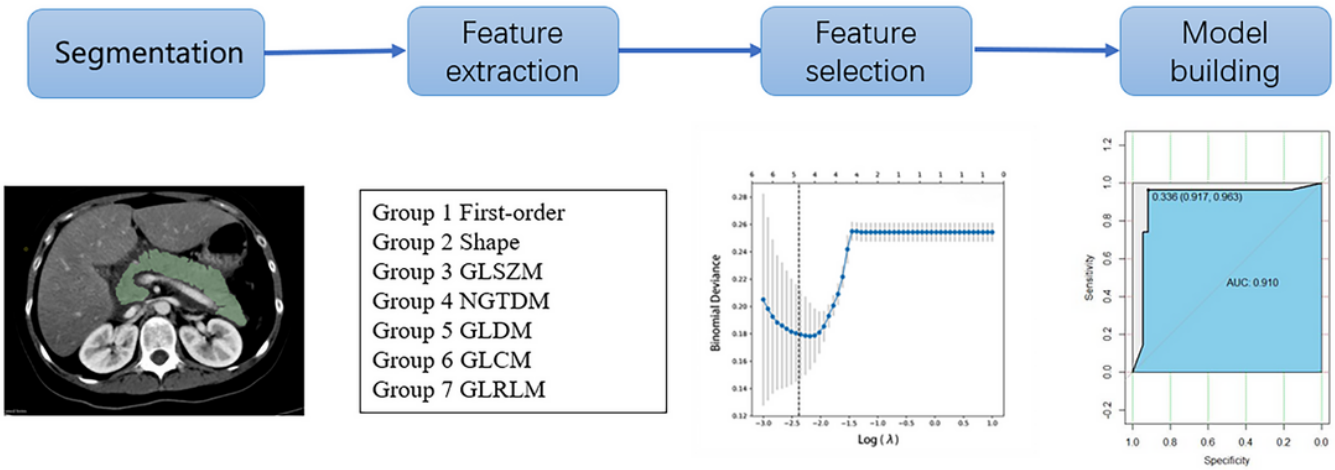

Figure 2

Workflow chart of the radiomic analysis

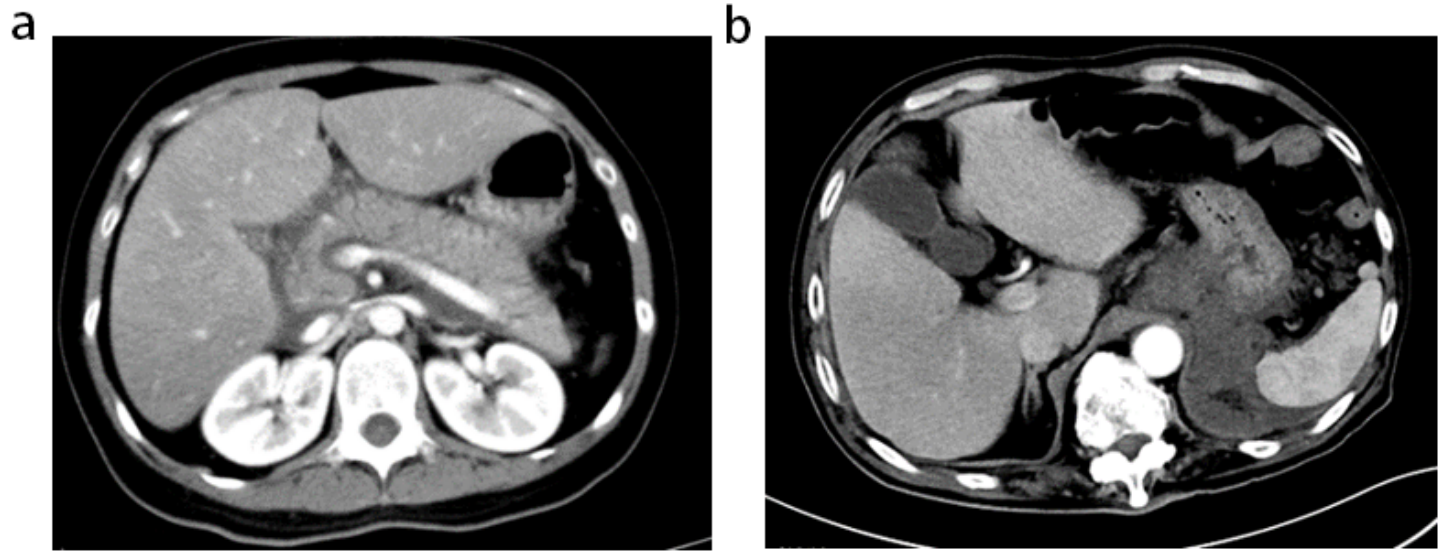

Figure 3

A CECT image of an AP patient without liver injury (a). The ALT, AST, TBIL, DBIL, MSCT, APACHE II, and BISAP scores were 13, 15, 16, 3.8, 4, 0, and 1, respectively. A CECT image of an AP patient with liver injury (b). The ALT, AST, TBIL, DBIL, MSCT, APACHE II, and BISAP scores were 126, 132, 20.9, 12.9, 10, 10, and 2, respectively. Moreover, there was no difference in the CECT between these two groups.

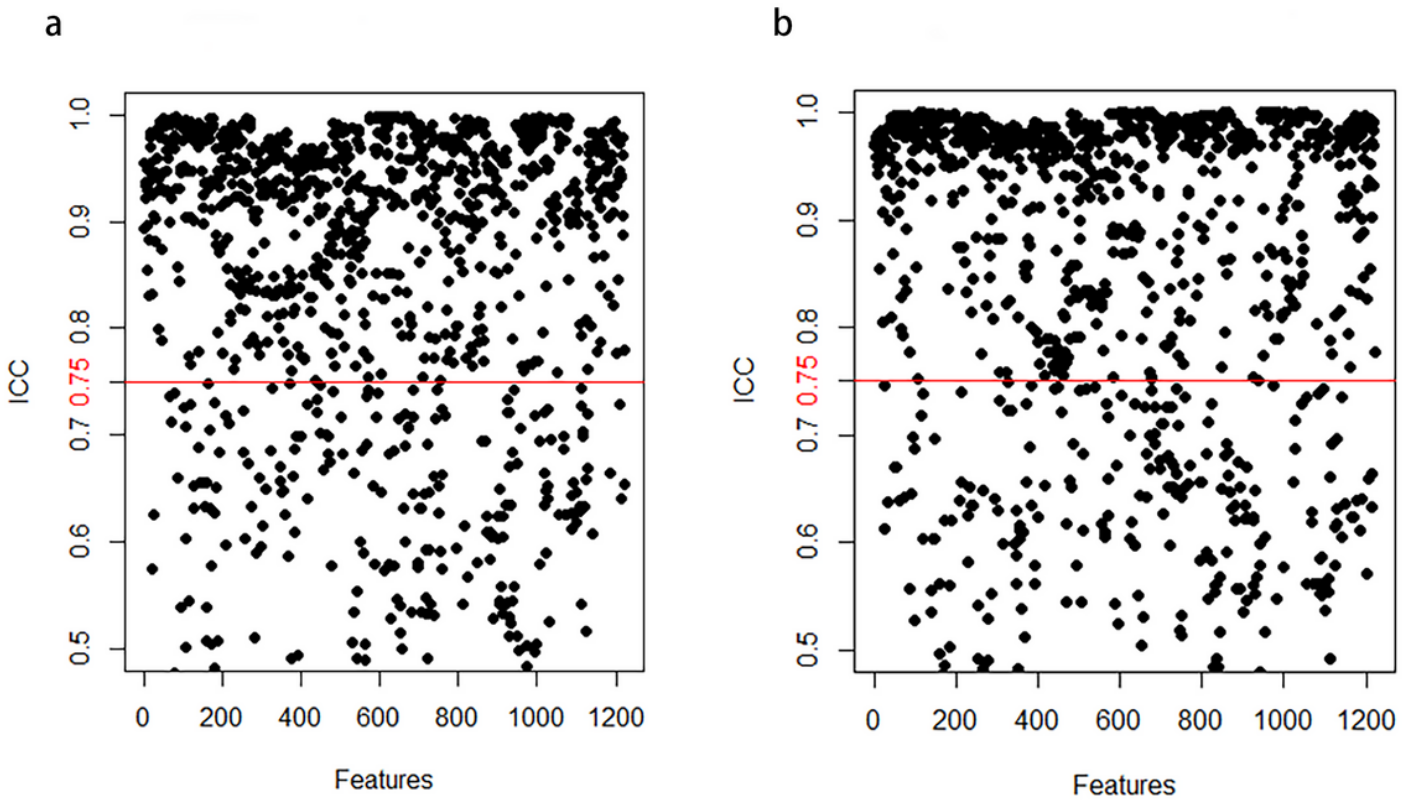

Figure 4

Consistency test of features. a. The intraobserver agreement based on the interclass correlation coefficient (ICC). b. Agreement of the interobserver agreement based on the ICC.

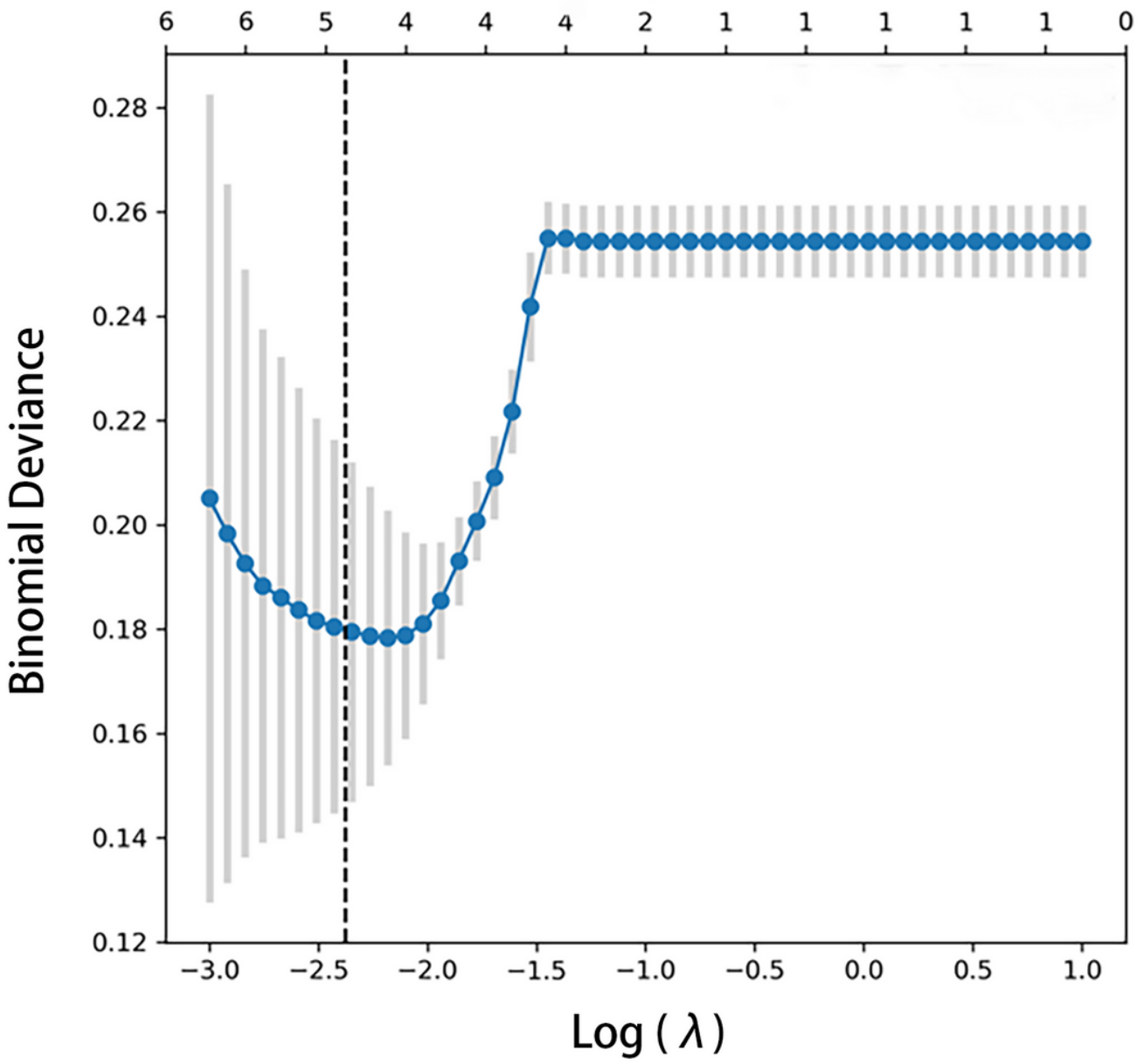

Figure 5

Feature selection using the least absolute shrinkage and selection operator (LASSO)

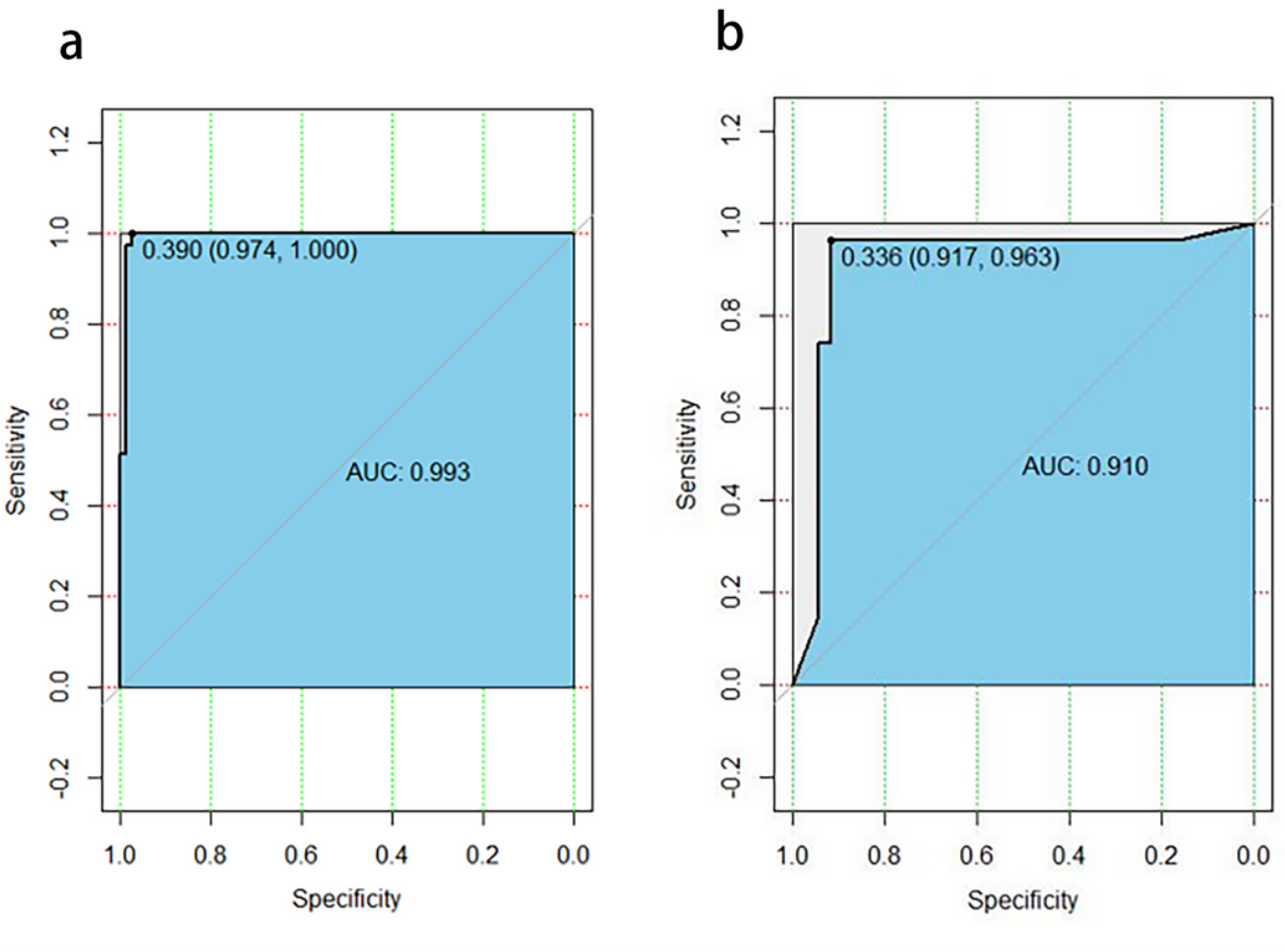

Figure 6

Performance of the radiomic model in the training cohort (a) and test cohort (b).

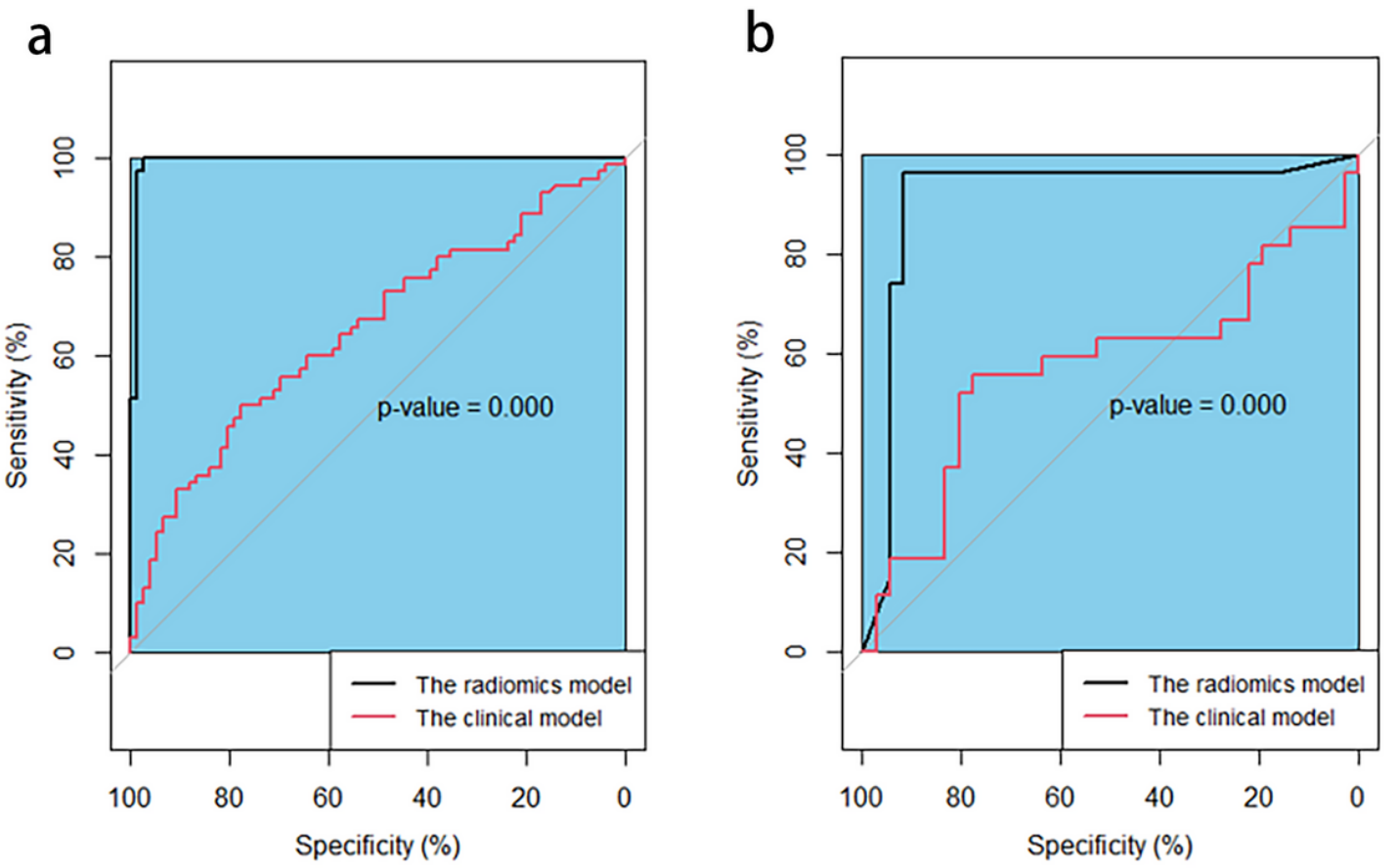

Figure 7

ROC curves comparing the radiomics model and clinical model between the training cohort (a) and the test cohort (b).